

Dynamics and Scaling of Noise-Induced Domain Growth

M. Ibañes¹, J. García-Ojalvo², R. Toral³, and J.M. Sancho¹

¹ Departament d'Estructura i Constituents de la Matèria, Universitat de Barcelona, Diagonal 647, E-08028 Barcelona, Spain

² Departament de Física i Enginyeria Nuclear, Universitat Politècnica de Catalunya, Colom 11, E-08222 Terrassa, Spain

³ Instituto Mediterráneo de Estudios Avanzados, IMEDEA (CSIC-UIB), Campus UIB, E-07071 Palma de Mallorca, Spain

April 26, 2024

Abstract. The domain growth processes originating from noise-induced nonequilibrium phase transitions are analyzed, both for non-conserved and conserved dynamics. The existence of a dynamical scaling regime is established in the two cases, and the corresponding growth laws are determined. The resulting universal dynamical scaling scenarios are those of Allen-Cahn and Lifshitz-Slyozov, respectively. Additionally, the effect of noise sources on the behaviour of the pair correlation function at short distances is studied.

PACS. 05.40.-a Fluctuation phenomena, random processes, noise, and Brownian motion – 64.60.-i General studies of phase transitions

1 Introduction

Growth processes for systems in their evolution towards a final state of thermodynamic equilibrium have been intensively studied during the last decades [1]. A particularly interesting situation concerns the case in which equilibrium corresponds to either of two equivalent phases of a scalar field $\phi(\mathbf{x}, t)$. Since in equilibrium the relevant free energy F is minimized, “equivalent” stands in this context for phases that have the same (minimum) value of that free energy. A typical case corresponds to the evolution following a sudden quench from a very high-temperature, homogeneous phase, to a final state below a critical temperature for an order-disorder transition. In this process, one can distinguish three regimes:

i) Right after the quench, the system finds itself out of equilibrium and small domains start to appear, corresponding to islands of each one of the two phases. The initial instability mechanism varies with the system.

ii) At late times, motion of the domain walls separating equivalent phases leads to a situation of domain growth, also known as *coarsening*. This regime occurs when the typical domain size $R(t)$ is much larger than the width of the interface between domains and much smaller than the system size. The main general mechanism for coarsening is the reduction of the excess of interfacial energy, which is accomplished by reducing the interface curvature. The exact details of the domain growth dynamics depend on the spatial dimension d and on the existence (or absence) of conservation laws. For dimension $d > 1$ and for a system whose order parameter is not conserved (i.e., which evolves towards a final one-phase, symmetry-breaking, equilibrium ordered state), the domain size $R(t)$ grows with time t as $R(t) \sim t^{1/2}$ (Allen-Cahn law). On the other hand,

for a system with a conserved order parameter (i.e., in which the final state has two coexisting phases), it has been found that $R(t) \sim t^{1/3}$ (Lifshitz-Slyozov law). Moreover, in both cases the relaxation of these systems towards equilibrium has been found to be self-similar. This claim basically states that, after the initial transient regime, the only relevant length scale is the domain size $R(t)$, so that two images of the system taken at two different times, t_1 and t_2 , can be made to match (in a statistical sense) by rescaling their lengths by $R(t_1)$ and $R(t_2)$, respectively. The validity of this *dynamical scaling law* [2,3] has a precise statement in terms of the correlation function, and has been extensively verified in many experiments, as well as in computer simulations of discrete and continuous models [1].

iii) Finally, when the domain size $R(t)$ is of the order of the system size, the system asymptotically reaches an equilibrium steady state, in which either only one of the two phases occupies the whole system (non-conserved order parameter case) or two large domains separated by a single boundary coexist (conserved order parameter case). In this case, the only relevant length scale of the problem is the equilibrium static correlation length.

Quite generally, the growth processes mentioned above have been described theoretically by the following dynamical equation:

$$\frac{\partial \phi(\mathbf{x}, t)}{\partial t} = -\Gamma \frac{\delta \mathcal{F}}{\delta \phi(\mathbf{x}, t)} + \eta(\mathbf{x}, t), \quad (1)$$

where $\mathcal{F}[\phi]$ is a suitable nonequilibrium free-energy functional, Γ is a kinetic coefficient and $\eta(\mathbf{x}, t)$ is a Gaussian white noise representing internal fluctuations, taken to

have zero mean and correlation:

$$\langle \eta(\mathbf{x}, t) \eta(\mathbf{x}', t') \rangle = 2 \varepsilon \delta(\mathbf{x} - \mathbf{x}') \delta(t - t'). \quad (2)$$

When $\epsilon = \Gamma k_B T$ (what is known as the fluctuation-dissipation relation), the system reaches an equilibrium state governed by the well-known Boltzmann–Gibbs distribution $\exp[-\mathcal{F}/k_B T]$. In the absence of fluctuations, the free-energy \mathcal{F} is a Lyapunov potential for the dynamical evolution, and the resulting dynamics is classified as potential [4]. It is worth stressing that the growth laws and dynamical scaling introduced before hold independently of the strength of the fluctuation terms, i.e. of the value of ϵ . This is true as far as those fluctuation terms are not extremely large (such that they inhibit the formation of order), or near a critical point (where fluctuations are largely amplified).

Most of the work in the past has dealt with the simpler case when the corresponding deterministic dynamics is potential. Only in last years, attention has been focused on more general dynamics where the final state is not of thermodynamic equilibrium. Most studies have been concerned with the case in which the deterministic dynamics does not imply the minimization of a free energy, the so-called non-potential dynamics [5]. New and interesting effects can appear in this case. For instance, it has been found that several stable phases can coexist in the system in a non-coarsening situation [6].

A new type of non-potential systems presenting order-disorder phase transitions has been introduced recently. The main feature of those systems is that the initial instability leading to domain growth and coarsening is induced by fluctuation terms of external origin. This is a rather counterintuitive effect of noise, in that an increase of the noise intensity can lead to a spatially ordered pattern. This phenomenon is nowadays well established and has lead to a host of new effects in which noise has a spatial ordering role (see [7] for a recent review). These effects include enlargement of the coexistence region in standard models of phase transitions [8], pure noise-induced phase transitions [9], noise-driven structures in pattern-formation processes [10], and noise-sustained pulse propagation [11], among others. In all these cases, a nonequilibrium ordered pattern can emerge as a consequence of the fluctuating terms, and disappears when the noise source is switched off. The final state cannot be made to correspond to any known free-energy, and the equivalence of the different phases can be established, whenever possible, by symmetry arguments. These systems can be described by the following Langevin equation

$$\frac{\partial \phi(\mathbf{x}, t)}{\partial t} = -\Gamma \left[\frac{\delta \mathcal{F}}{\delta \phi(\mathbf{x}, t)} + g(\phi) \xi(\mathbf{x}, t) \right] + \eta(\mathbf{x}, t), \quad (3)$$

where $\xi(\mathbf{x}, t)$ represents external fluctuation sources (multiplicative noise, if g depends on ϕ), to be characterized statistically (see later).

So far, studies of noise-induced spatial order have been concerned with the characterization of the final, nonequilibrium steady state (which would correspond to regime

(iii) above). In particular, much effort has been devoted to determine the phase diagram and the critical properties of these systems, including the possible existence of new universality classes for the steady state. A great deal of our knowledge of the detailed behaviour of these systems comes from numerical simulations of the corresponding stochastic partial differential equations. On the theoretical side, studies have used mean-field theories, dynamic renormalization group, and linear stability analyses [7]. Renormalization-group arguments, for instance, show that multiplicative noise is less relevant than additive noise, when both are present, to the universal behaviour, and thus it does not change the universality of the resulting critical points [7]. In this paper, on the other hand, we are concerned with the noise-induced *dynamical* evolution of both conserved and non-conserved systems towards a nonequilibrium steady state (which would correspond to the scaling regime (ii) defined above). We will be interested in studying the growth laws and whether dynamical scaling holds in these cases.

This paper is organized in the following way. In section II we study numerically the scaling properties and the growth of domains for the two-dimensional *non-conserved* Ginzburg–Landau model in presence of both external and internal fluctuations. In section III we characterize numerically the phase separation dynamics induced by external noise in the two-dimensional *conserved* Ginzburg–Landau model. Finally, section III is devoted to the study of the pair correlation function at short distances in the presence of noise sources.

2 Non-conserved model

As stated in the introduction, when a system in a high-temperature disordered equilibrium state is quenched below its order-disorder transition temperature, for which equivalent ordered phases can coexist, domains of the new equilibrium phases appear and grow. For those systems whose order parameter is not conserved, one of the domains grows until it fills the whole system, assumed finite. The domain boundaries move with a translational velocity that has been found, for spatial dimension $d \geq 2$, to be basically proportional to the mean curvature of the boundaries, and independent of the free energy of the interface. This mechanism leads to the well-known Allen–Cahn law for the growth of the average linear size $R(t)$ of phase domains: $R(t) \propto t^{1/2}$. The same law, with a different physical mechanism, has been shown to hold in other models as well [12].

A particular model for which the above results have been established is the non-conserved Ginzburg–Landau model (known as model A in the literature of critical phenomena [13]). It is defined by Eq. (1) with a constant kinetic coefficient $\Gamma = 1$, and with the following free energy:

$$\mathcal{F} = \int d\mathbf{x} \left[-\frac{a}{2} \phi^2 + \frac{1}{4} \phi^4 + \frac{D}{2} |\nabla \phi|^2 \right]. \quad (4)$$

For fixed values of the diffusion constant D and the internal noise strength ϵ , there is a critical value $a_c(D, \epsilon)$ such that for $a < a_c$ equilibrium corresponds to a single homogeneous phase (the *disordered* phase), whereas for $a > a_c$ two equivalent equilibrium phases (with the same minimum value of the free energy) coexist. Due to the symmetry of \mathcal{F} , the *ordered* phases are related by a global change of sign of the field ϕ . The critical value a_c vanishes for zero noise intensity $a_c(D, \epsilon = 0) = 0$.

A new ordering situation can arise if we let fluctuate the control parameter $a \rightarrow a + \xi(\mathbf{x}, t)$. Even when the mean value of a is still below the critical level $\langle a \rangle < a_c$, it might be possible, by choosing a sufficiently large intensity of the external fluctuations, to have a bistable stationary (but no longer equilibrium) distribution for the field. The two maxima of the stationary distribution are again symmetric under a global change of sign.

In the presence of both internal and external fluctuations, the non-conserved Ginzburg–Landau model is obtained by substitution of the free energy functional (4) in the Langevin equation (3). One finds

$$\frac{\partial \phi(\mathbf{x}, t)}{\partial t} = a\phi - \phi^3 + D \nabla^2 \phi + \phi \xi(\mathbf{x}, t) + \eta(\mathbf{x}, t), \quad (5)$$

where both additive and multiplicative noises are Gaussian, with zero mean. The additive-noise correlation is defined by Eq. (2). In general, the external multiplicative noise $\xi(\mathbf{x}, t)$ may have specific temporal and spatial correlation functions. For the moment, we will assume that:

$$\langle \xi(\mathbf{x}, t) \xi(\mathbf{x}', t') \rangle = 2 \sigma^2 c(\mathbf{x} - \mathbf{x}') \delta(t - t'), \quad (6)$$

i.e. a delta-correlated function in time and a general correlation function $c(\mathbf{x})$ in space. In this case, for given ϵ and D , the critical value of a depends on σ in such a way that its value is *lowered* with respect to the case with no external fluctuations, $\sigma = 0$. In the limit of small ϵ , a linear stability analysis [14,15] and a mean-field type theory [16,17] give the approximate result $a_c = -\sigma^2 c(0)$. Since ordered states appear for $a > a_c$, by choosing parameter values satisfying $-\sigma^2 c(0) < a < 0$ we have a situation in which nonequilibrium steady phases *induced by external noise* appear and grow (see Fig. 1). If external fluctuations are switched off the ordered state disappears, since the (negative) value of a is now below the critical value. In this section, we want to elucidate if the growth of these domains still follows the Allen–Cahn law and if the system still exhibits a scaling regime.

Most of the results of this section have been obtained by a numerical integration of the stochastic model defined by Eq. (5). In order to perform the numerical analysis, we redefine the model by considering a regular d -dimensional lattice with N^d points and lattice spacing Δx :

$$\frac{d\phi_i}{dt} = a\phi_i - \phi_i^3 + D \sum_j \tilde{D}_{ij} \phi_j + \eta_i(t) + \phi_i \xi_i(t), \quad (7)$$

where $\phi_i(t) \equiv \phi(\mathbf{x}_i, t)$ and only one index is used to label the cells, independently of the dimension of the lattice.

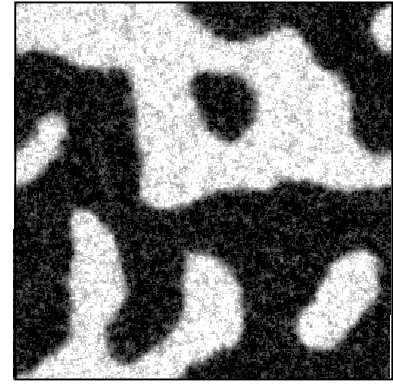


Fig. 1. Spatial pattern for the stochastic model A with $\sigma^2 = 0.4$, $\epsilon = 10^{-4}$, $a = -0.2$, and $D = 1$ at $t=200$. The square lattice has 256×256 cells of mesh size $\Delta x = 1$. The black and white domains correspond to symmetric phases.

\tilde{D}_{ij} accounts for the discrete Laplacian operator

$$\nabla^2 \rightarrow \sum_j \tilde{D}_{ij} = \frac{1}{(\Delta x)^2} \sum_j (\delta_{nn(i),j} - 2d \delta_{i,j}), \quad (8)$$

where $nn(i)$ represents the set of all the sites that are nearest neighbors of site i . The discrete noises $\eta_i(t)$ and $\xi_i(t)$ are still Gaussian with zero mean and correlations

$$\langle \eta_i(t) \eta_j(t') \rangle = 2 \varepsilon \frac{\delta_{i,j}}{(\Delta x)^d} \delta(t - t') \quad (9)$$

and

$$\langle \xi_i(t) \xi_j(t') \rangle = 2 \sigma^2 \frac{\delta_{i,j}}{(\Delta x)^d} \delta(t - t'). \quad (10)$$

This last expression corresponds to an external noise with a white spatial correlation in the lattice, i.e. $c(0) = 1/\Delta x^d$. Since we will choose $\Delta x = 1$ in all the results shown in the paper, $c(0) = 1$ in what follows.

After the discretization procedure described above, the resulting set of coupled stochastic differential equations for the variables ϕ_1, \dots, ϕ_N has been integrated numerically. We have studied two cases of noise-induced non-conserved dynamics, corresponding to two different multiplicative noise intensities, $\sigma^2 = 0.4$ and $\sigma^2 = 0.6$. In both cases, the additive noise intensity is $\epsilon = 10^{-4}$, and $a = -0.2$. Since these values satisfy $-\sigma^2 < a < 0$, the linear stability analysis indicates that the homogeneous state is unstable for these multiplicative noise intensities [14,15]. We have compared these two cases with the purely deterministic model $\varepsilon = \sigma = 0$ for $a = 1$, and with the stochastic model with only additive noise ($\sigma = 0$) for $a = 2$ and $\epsilon = 0.7$. In all cases we have chosen the coupling coefficient to be $D = 1$.

Our numerical analysis has been performed in a two-dimensional square lattice of 256×256 cells with periodic boundary conditions and mesh size $\Delta x = 1$, except for

the stochastic model with only additive noise, which has been considered in a lattice of 128×128 cells in order to compare with the results of Ref. [18]. We have used a first-order Euler algorithm with a time step $dt = 10^{-2}$ in the deterministic case, and $dt = 5 \cdot 10^{-3}$ in presence of noise sources. The noises have been generated using a numerical inversion method [19]. As initial condition, we have chosen in all cases a random uniform distribution of the field in the interval $(-1, 1)$ in order to simulate a high-temperature one-phase state. Our results are averaged over 15 samples in the deterministic case, 40 samples in the purely additive-noise case, and 30 samples in the two multiplicative-noise cases.

In order to study the growth process and to examine the existence of dynamical scaling, we define the correlation and structure functions. These two functions give information about the spatial structure of the system at a certain time. By knowing how these functions evolve, one can obtain information about the growth of domains, and check if there is a scaling regime. In our discrete space, we define the pair correlation function as:

$$G(\mathbf{r}_j, t) = \left\langle \frac{1}{N^d} \sum_i \phi(\mathbf{r}_j + \mathbf{x}_i, t) \phi(\mathbf{x}_i, t) \right\rangle \quad (11)$$

where the brackets denote an average over different initial conditions and realizations of the noises.

The structure function is the (discrete) Fourier transform of the pair correlation function:

$$S(\mathbf{k}_\mu, t) = (\Delta x)^d \sum_j e^{-i\mathbf{r}_j \cdot \mathbf{k}_\mu} G(\mathbf{r}_j, t), \quad (12)$$

where μ labels the N^d points in Fourier space.

In practice, the structure function is computed in an easier way using the equivalent definition

$$\hat{\phi}(\mathbf{k}_\mu, t) = \frac{1}{\Delta x^d N^d} \langle |\hat{\phi}(\mathbf{k}_\mu, t)|^2 \rangle, \quad (13)$$

in terms of the Fourier transform of the field:

$$\hat{\phi}(\mathbf{k}_\mu, t) = (\Delta x)^d \sum_j e^{-i\mathbf{r}_j \cdot \mathbf{k}_\mu} \phi(\mathbf{r}_j, t), \quad (14)$$

and the correlation function $G(\mathbf{r}_i, t)$ is then computed as the inverse Fourier transform of $S(\mathbf{k}_\mu, t)$.

We perform a spherical average of the pair correlation and structure functions

$$G(r, t) = \frac{1}{N_r} \sum_{r \leq r_i < r + \Delta r} G(\mathbf{r}_i, t) \quad (15)$$

$$S(k, t) = \frac{1}{N_k} \sum_{k \leq k_\mu < k + \Delta k} S(\mathbf{k}_\mu, t), \quad (16)$$

where the sums run over the set of lattice points (N_r and N_k) between two circles of radius r and $r + \Delta r$, or k and $k + \Delta k$, in real and reciprocal space, respectively.

Finally, in order to compare results from different parameter values, we have used the following normalization

$$g(r, t) = \frac{G(r, t)}{G(0, t)}, \quad s(k, t) = \frac{S(k, t)}{G(0, t)}. \quad (17)$$

When the interface between domains is very thin compared with their size, the system has a single characteristic length $R(t)$, which is related to the average size of domains. The scaling hypothesis states that the pair correlation function depends on time only through the time-dependent characteristic length:

$$g(r, t) = g(r/R(t)) \quad (18)$$

The length $R(t)$ can be defined in several ways, but in the scaling regime all of them should lead to the same law for domain growth. We have chosen $R(t)$ as the distance at which the pair correlation function is half its maximum value, i.e. $g(R(t), t) = 1/2$. Since the structure factor is the Fourier transform of the correlation function, we derive its scaling law as

$$s(k, t) = R(t)^d s(kR(t)) \quad (19)$$

with no other explicit dependence on time.

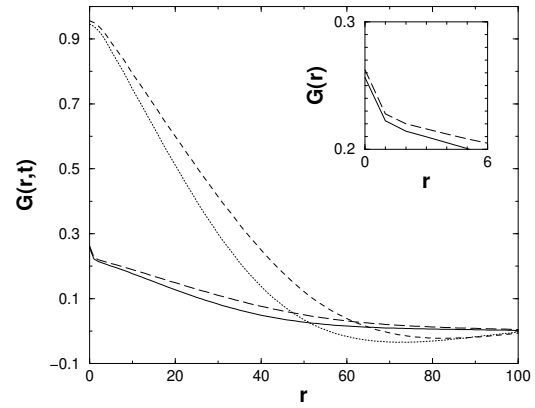


Fig. 2. Pair correlation function for the 2-dimensional non-conserved Ginzburg-Landau model in the deterministic and stochastic cases. The dotted ($t=300$) and dashed ($t=500$) lines correspond to the deterministic case with $a = 1$ and $D = 1$. The solid ($t=300$) and the long-dashed ($t=500$) lines correspond to the stochastic model with $\epsilon = 10^{-4}$, $\sigma^2 = 0.6$, $a = -0.2$ and $D = 1$. In presence of noise sources the pair correlation function exhibits a peak at $r = 0$, as shown more clearly in the inset.

We plot in Fig. 2 the pair correlation function for the deterministic case with $a = 1$ and for the nonequilibrium stochastic case with $\sigma^2 = 0.6$, $a = -0.2$, for two different times. As time increases, the correlation function tends to a monotonically decreasing function with an increasing characteristic decay length. A closer look (see inset of Fig. 2) shows that in the stochastic case the pair correlation function is not smooth near the origin. This behaviour

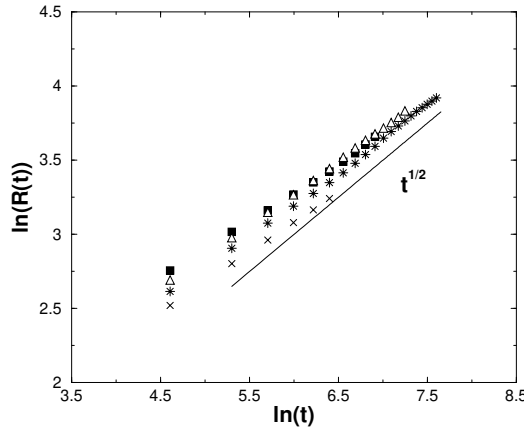


Fig. 3. The Allen-Cahn law. Stars correspond to the deterministic model with $a = 1$ and $d = 1$. Crosses correspond to the additive case ($\epsilon = 0.7$, $a = 2$ and $D = 1$), squares to $\sigma^2 = 0.4$, and triangles to $\sigma^2 = 0.6$. The two cases with multiplicative noise have $\epsilon = 10^{-4}$, $a = -0.2$ and $D = 1$. The solid line is a guide to the eye.

at short distances appears whenever noise sources (either multiplicative or additive) exist, and it differs from what is observed in the deterministic case, where the pair correlation function is smooth at all distances. As we will see, this behaviour is a bulk feature and, since it does not present scaling, we have avoided it in the following section by substituting $G(r, t)$ near $r = 0$ by a parabolic fit. The last section is devoted to the understanding of the behaviour of the pair correlation function at short distances in the presence of noise sources.

Figure 3 shows the square root dependence on time of the average domain size. The Allen-Cahn law is seen to be verified by all models under study. The prefactor seems to depend on the noise intensity.

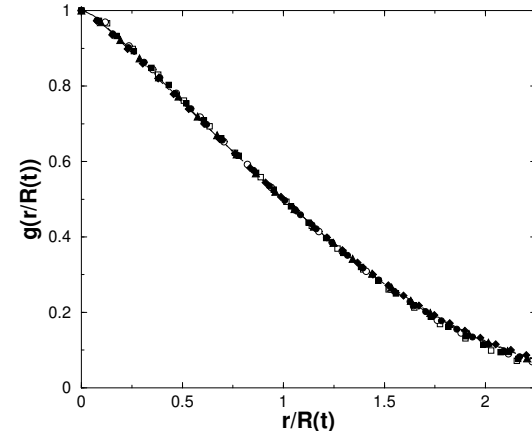
Numerical results for the scaled pair correlation and the structure functions are shown in Figs. 4(a) and 4(b), respectively. Our numerical simulations verify scaling for both the pair correlation and the structure functions. Furthermore, the observed scaled structure functions agree with the theoretical prediction of Ref. [20], which has two adjustable parameters (a scale factor in each axis), and are also in agreement with Ref. [18].

3 Conserved Model

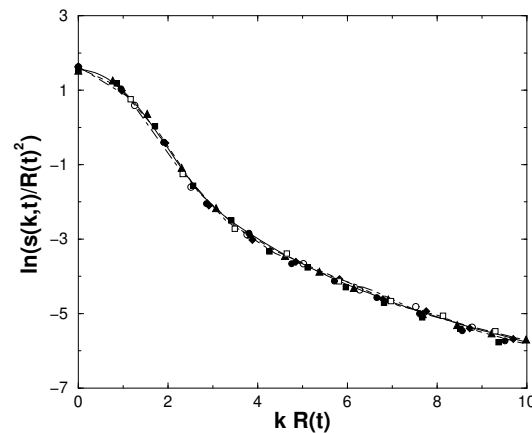
The conserved version of the model studied in the previous section, Eq. (5), is

$$\frac{\partial \phi(\mathbf{x}, t)}{\partial t} = -\nabla^2 [a\phi - \phi^3 + D \nabla^2 \phi + \phi \xi(\mathbf{x}, t)] + \eta(\mathbf{x}, t), \quad (20)$$

which in the absence of external noise is the Cahn-Hilliard-Cook model [21] and in the literature of critical phenomena [13] is known as model B. The conservation law is $V^{-1} \int_V d\mathbf{x} \phi(\mathbf{x}, t) = \phi_0$, constant, where V is the total volume of the system. This constant is given by the initial



(a)



(b)

Fig. 4. Scaled pair correlation function (a) and structure function (b) for the non-conserved Ginzburg-Landau model. Broken lines correspond to the deterministic model with $a = 1$ and $D = 1$ for $t=1000$ (dashed line) and $t=1500$ (dot-dashed line). Empty symbols, squares ($t=500$) and circles ($t=600$), correspond to the additive model ($\epsilon = 0.7$, $a = 2$ and $D = 1$). Full symbols correspond to the nonequilibrium models. Squares ($t=800$) and circles ($t=1000$) correspond to $\sigma^2 = 0.4$, while triangles ($t=600$) and diamonds ($t=1000$) correspond to $\sigma^2 = 0.6$. Both cases have $a = -0.2$, $D = 1$ and $\epsilon = 10^{-4}$. The continuous line in (b) is the theoretical prediction of Ohta et al. [20].

volume fraction of the system. This conserved model is suitable for the description of the evolution of systems such as binary alloys, in which the total concentration of each component of the alloy is kept constant. In this case, the local order parameter, $\phi(\mathbf{x}, t)$ represents the local difference of concentrations of each component of the alloy. As before, we consider external fluctuations on the control parameter a . Both additive and multiplicative noises are Gaussian, with zero mean and correlation given by

$$\langle \eta(\mathbf{x}, t) \eta(\mathbf{x}, t') \rangle = -2 \epsilon \nabla^2 \delta(\mathbf{x} - \mathbf{x}') \delta(t - t'). \quad (21)$$

and Eq. (6). The Laplacian term in Eq. (21) ensures that in absence of multiplicative noise and if $\epsilon = k_B T$ (the fluctuation-dissipation theorem), the stationary distribution is still governed by a (restricted) Boltzmann-Gibbs distribution $\exp[-\mathcal{F}/k_B T] \delta(V^{-1} \int_V d\mathbf{x} \phi(\mathbf{x}, t) - \phi_0)$. Let us consider this equilibrium conserved model in a high-temperature, disordered, one-phase state corresponding to a sufficiently low value of the parameter a . If we now suddenly decrease the temperature of the system below its transition value (equivalently, by increasing a), the disordered one-phase state becomes unstable and the system develops domains of the new phases which slowly tend to the equilibrium ones. The classical theory of the kinetics of first order phase transitions distinguishes two regimes for the initial instability leading to coarsening: for a quench taking the system deep inside the coexistence curve (critical quench or small order parameter ϕ_0) the system is unstable against long-wavelength perturbations and undergoes a process of spinodal decomposition. On the other hand, for quenches close to the coexistence curve, the system evolves by nucleation and growth of the nuclei formed. In any case, since the order parameter is conserved, the growth of a given domain is at expense of the smaller domains of the same phase. Domain growth appears as a result of diffusion across the interface between domains, caused by the interface curvature. The equilibrium final state is a two-phase coexisting state. In this time regime, the average domain size grows with time as $R(t) \propto t^{1/3}$, which is called the Lifshitz-Slyozov law. This power-law behaviour has been derived analytically for small volume fractions, although it has been seen numerically to be also satisfied even for large volume fractions [22]. As in the non-conserved case, when the growth of domains verifies the corresponding power-law behaviour, the pair correlation function and the structure function satisfy the scaling hypothesis defined in Eq. (18). The scaled functions have not been analytically obtained so far.

In this section we are concerned with the dynamics towards the nonequilibrium, two-phase coexisting steady state induced by external fluctuations. Let us now consider the above nonequilibrium model [Eq. (20)] in a disordered, $\phi_0 = 0$, one-phase steady state corresponding to a small intensity of the multiplicative noise. If we now increase abruptly the intensity of the external fluctuations, σ , the system develops domains of new phases that grow and tend to the new stationary values (see Fig. 5). For an external noise with a white spatial correlation in the lattice ($c(0) = 1$, as in the previous section), a linear stability analysis [23] shows that order appears in this case for values for a above a critical point $a_c = -2d\sigma^2$. Hence, for $-2d\sigma^2 < a < 0$, phase separation induced by fluctuations appears. We will now address the issue of whether this dynamics still verifies the Lifshitz-Slyozov law, and whether a scaling behaviour for the pair correlation and structure functions exists.

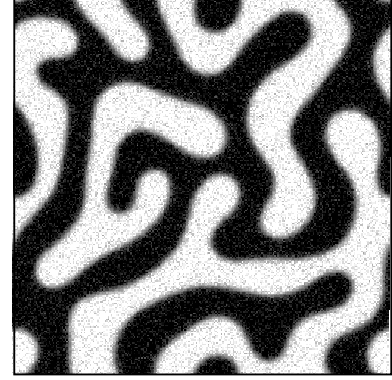


Fig. 5. Spatial pattern for the stochastic model B at $t=10000$, with multiplicative noise intensity $\sigma^2 = 0.1$, $\epsilon = 10^{-4}$, $a = -0.2$, $D = 1$ and $\phi_0 = 0$. The square lattice has 256×256 cells of mesh size $\Delta x = 1$. The black and white domains correspond to symmetric phases.

As in the previous section, we define the model [given by Eq. (20)] in a discrete space of mesh size Δx

$$\frac{d\phi_i}{dt} = - \sum_k \tilde{D}_{ik} \left[a \phi_k - \phi_k^3 + D \sum_j \tilde{D}_{kj} \phi_j + \phi_k \xi_k(t) \right] + \eta_k(t) \quad (22)$$

The discrete noises $\eta_i(t)$ and $\xi_i(t)$ are still Gaussian, with zero mean and correlations given by

$$\langle \eta_i(t) \eta_j(t') \rangle = -2 \varepsilon \frac{\tilde{D}_{i,j}}{\Delta x^d} \delta(t - t') \quad (23)$$

and Eq. (10). These conserved noise term $\eta_i(t)$ can be generated as the divergence of a stochastic vector field [24].

We have studied two cases of noise-induced conserved dynamics corresponding to two different intensities of the multiplicative noise, $\sigma^2 = 0.1$ and $\sigma^2 = 0.2$. In both cases, additive noise is $\epsilon = 10^{-4}$ and the control parameter is $a = -0.2$, which corresponds to a situation in which the disordered state, $\phi_i = 0 \forall i$, is the deterministically stable phase. However, since $-4\sigma^2 < a < 0$, it turns out that for these multiplicative noise intensities, the one-phase disordered state becomes unstable [15]. We have compared their behaviour with three equilibrium cases: the purely deterministic model for $a = 2$ and $a = 0.2$, and the stochastic model B with only additive noise ($\sigma = 0$, $a = 2$ and $\epsilon = 0.7$). In all cases we have taken the coupling coefficient as $D = 1$.

We have performed numerical simulations of the full model in a two dimensional regular square lattice of 256×256 points with periodic boundary conditions and mesh

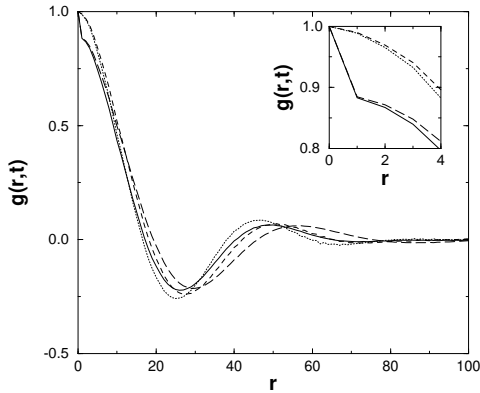


Fig. 6. Normalised pair correlation function for the 2-dimensional conserved model in the deterministic and nonequilibrium stochastic cases. The dotted ($t=7000$) and dashed ($t=10000$) lines correspond to the deterministic case with $a=2$ and $D=1$. The solid ($t=7000$) and the long-dashed ($t=10000$) lines correspond to the stochastic model with $\epsilon=10^{-4}$, $\sigma^2=0.1$, $a=-0.2$ and $D=1$. In presence of noise sources, the pair correlation function is not smooth at short distances, as seen more clearly in the inset. In both cases we have considered $\phi_0=0$.

size $\Delta x = 1$. Since the model is self-averaging and the size we have chosen is relatively large, it has not been necessary to consider many different realizations in order to have small statistical errors. In particular, we have calculated averages over up to 6 realizations for the equilibrium models, and over 10 realizations for the nonequilibrium stochastic models with multiplicative noise. We have implemented a first-order Euler algorithm and used a time step of $dt = 10^{-2}$ in the deterministic case and $dt = 5 \cdot 10^{-3}$ in presence of noise sources. As initial conditions we have considered a Gaussian random field with zero mean and variance 10^{-2} ($\phi_0 = 0$).

The definition of the pair correlation function and the structure factor are the same as in the non-conserved case. The only difference is that now the spatial average of $\phi(\mathbf{x}, t)$ is a constant determined by the initial condition. The pair-correlation function oscillates and decays to zero with a characteristic distance that is a measure of the typical domain size. This is shown in Fig. 6, where we plot the evolution of the pair correlation function for the deterministic ($a = 0.2$) and stochastic ($\epsilon = 10^{-4}$, $\sigma^2 = 0.1$, $a = -0.2$) cases. The first zero crossing defines the growth length, $g(R(t), t) = 0$. As in the non-conserved case, we have also found the same behaviour of the correlation function at short distances that differs from what is observed in the deterministic case (see inset of Fig. 6). We have proceeded in a similar way as before by using a parabolic fit of $G(r, t)$ at $r = 0$.

As shown in Fig. 7, our numerical results indicate that the average domain size obeys the equilibrium Lifshitz-Slyozov law even in the presence of multiplicative noise. The corresponding scaled pair correlation and structure

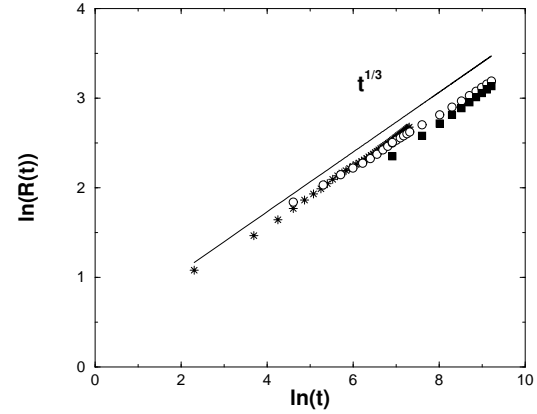


Fig. 7. Average domain size $R(t)$ for the conserved model. Stars correspond to the deterministic case with $a = 2$ and empty circles to the stochastic equilibrium model with $a = 2$ and $\epsilon = 0.7$. Full squares correspond to the nonequilibrium stochastic model with $\sigma^2 = 0.2$, $\epsilon = 10^{-4}$ and $a = -0.2$. The solid line is a guide to the eye. In all cases the Lifshitz-Slyozov power law behaviour seems to be satisfied.

functions are plotted in Figs. 8(a) and 8(b). The scaling behaviour is seen to be verified by the nonequilibrium model with $\sigma^2 = 0.2$. Furthermore, the scaled functions agree with the equilibrium ones.

4 Noise Effects on the Short-Distance Behaviour of the Correlation Function

As we have seen in the previous sections, the discrete two-point correlation function of systems undergoing domain growth in the presence of fluctuations is not smooth at short distances, for both conserved and non-conserved dynamics (Figs. 2 and 6). This generic feature can be found in the existing literature [25], but as far as we know, it has not been explained yet. As we will see in this section, this behaviour is mainly a bulk feature, and the interfaces do not play any role. Therefore, it can be studied considering the bulk stationary situation.

4.1 Non-conserved Model

We intend to show that the presence of fluctuations in the steady bulk solution is responsible for the non-smooth behaviour of the discrete correlation function. To that end, we linearize the model given by Eq. (5) around the bulk phase, which, in order to simplify the analysis, we take as the homogeneous null phase ($\phi = 0$). Let us start with the non-conserved model with only additive noise, and linearize it around $\phi = 0$

$$\frac{\partial \phi(\mathbf{x}, t)}{\partial t} = a\phi + D \nabla^2 \phi + \eta(\mathbf{x}, t), \quad (24)$$

where the additive noise has zero mean and correlations given by Eq. (2). The stability of this model requires a to

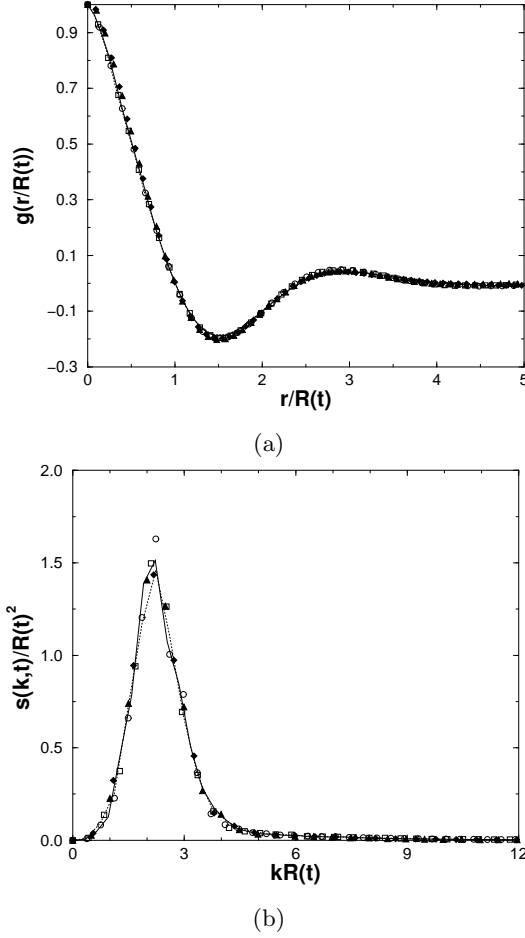


Fig. 8. Scaled pair correlation function (a) and scaled structure function (b) for the conserved model. Lines correspond to the deterministic model with $a = 2$ for $t = 1000$ (continuous line) and $t = 1600$ (dashed line). Empty symbols correspond to the equilibrium stochastic model with additive noise ($a = 2$ and $\epsilon = 0.7$) for $t = 2000$ (circles) and $t = 3000$ (squares). Full symbols correspond to the nonequilibrium stochastic model with $\sigma^2 = 0.2$, $\epsilon = 10^{-4}$ and $a = -0.2$ for $t = 7000$ (triangles) and $t = 9000$ (diamonds). In all cases $D = 1$ and $\phi_0 = 0$.

be negative. We now look for the dynamical equation of the pair-correlation function $G(\mathbf{r}, t)$, defined as the continuum version of (11) ($\mathbf{r} = \mathbf{x} - \mathbf{x}'$) [1]:

$$\frac{\partial G(\mathbf{r}, t)}{\partial t} = 2a G(\mathbf{r}, t) + 2D \nabla^2 G(\mathbf{r}, t) + 2\epsilon \delta(\mathbf{r}), \quad (25)$$

which has a delta contribution due to additive noise. In the stationary state, this equation can be solved in a straightforward way in Fourier space. The resulting integral is divergent in $d = 2$, indicating the absence of a continuum limit in this case. On the other hand, the integral converges in $d = 1$. Numerical simulations of Eq. (24) [see Fig. 9(a)] show a strong dependence on the noise intensity of the slope of the correlation function at $r = 0$. Therefore, this is a non-scaling feature, which can be characterized by studying the spatial derivative of $G(r, t)$ near the origin.

From (25), we obtain

$$\frac{d}{dr} G(r, t) \Big|_{r=0^+} = -\frac{\epsilon}{2D}, \quad (26)$$

where we have taken into account that the pair correlation function is symmetric, $G(\mathbf{r}, t) = G(-\mathbf{r}, t)$. This expression shows clearly the relevance of the noise intensity ϵ .

After this back-of-the-envelope calculation, we perform a more exhaustive analysis in discrete space, in order to compare it with the numerical results shown in Fig. 9(a). We now consider both additive and multiplicative noise sources and take the bulk phase $\phi = 0$. Thus, we linearize Eq. (7) around this phase and obtain

$$\frac{d\phi_i}{dt} = a\phi_i + D \sum_j \tilde{D}_{ij} \phi_j + \phi_i \xi_i(t) + \eta_i(t). \quad (27)$$

From this equation, and making use of Novikov's theorem [7], we can obtain the dynamical equation for the discrete correlation $\langle \phi_i(t) \phi_j(t) \rangle$:

$$\frac{d}{dt} \langle \phi_i(t) \phi_j(t) \rangle = 2a \langle \phi_i \phi_j \rangle + D \sum_k \left(\tilde{D}_{ik} \langle \phi_j \phi_k \rangle + \tilde{D}_{jk} \langle \phi_i \phi_k \rangle \right) + 2\sigma^2 \langle \phi_i \phi_j \rangle \frac{\delta_{ii} + \delta_{jj}}{\Delta x^d} + 2\epsilon \frac{\delta_{ij}}{\Delta x^d}. \quad (28)$$

Since we are analyzing a bulk feature, the dynamics is no longer relevant, and we can perform our calculations in steady state. Therefore, we set $\frac{d}{dt} \langle \phi_i(t) \phi_j(t) \rangle = 0$, for any i and j . Since we are interested on very short distances, we focus on $i = j$, to obtain:

$$a \langle \phi_i^2 \rangle + \frac{D}{\Delta x^2} \sum_{nn(i)} (\langle \phi_i \phi_{nn(i)} \rangle - \langle \phi_i^2 \rangle) + 2 \frac{\sigma^2}{\Delta x^d} \langle \phi_i^2 \rangle + \frac{\epsilon}{\Delta x^d} = 0, \quad (29)$$

where the Laplacian term has been made explicit and the sum runs over the $2d$ nearest neighbors of i .

In discrete space, the first derivative of the two-point correlation function $G_i \equiv G(\mathbf{r}_i)$ at $i = 0$ is

$$G'_0 \equiv \frac{\langle \phi_i \phi_{nn(i)} \rangle - \langle \phi_i^2 \rangle}{\Delta x}. \quad (30)$$

Taking into account the isotropy of the system, we have

$$\langle \phi_i \phi_{nn(i)} \rangle = G_1, \quad \forall nn(i) \quad (31)$$

where G_1 is the two-point correlation function for distances equal to one cell.

Considering Eqs. (30) and (31), expression (29) can be rewritten in the following form

$$G'_0 = -\frac{a}{2dD} \Delta x G_0 - \frac{\sigma^2}{dD \Delta x^{d-1}} G_0 - \frac{\epsilon}{2dD \Delta x^{d-1}}. \quad (32)$$

If we now take the continuous limit $\Delta x \rightarrow 0$ and consider that only additive noise is present ($\sigma^2 = 0$), we recover the continuous result (26) given above in the case of $d = 1$.

The numerical simulations shown in Fig. 9(a) have been performed on a one-dimensional lattice of $N = 16384$ points and mesh size $\Delta x = 1$, for $a = -2$ and $D = 1$. We have used a first-order Euler scheme with $dt = 5 \cdot 10^{-3}$, and computed the two-point correlation function in the stationary state.

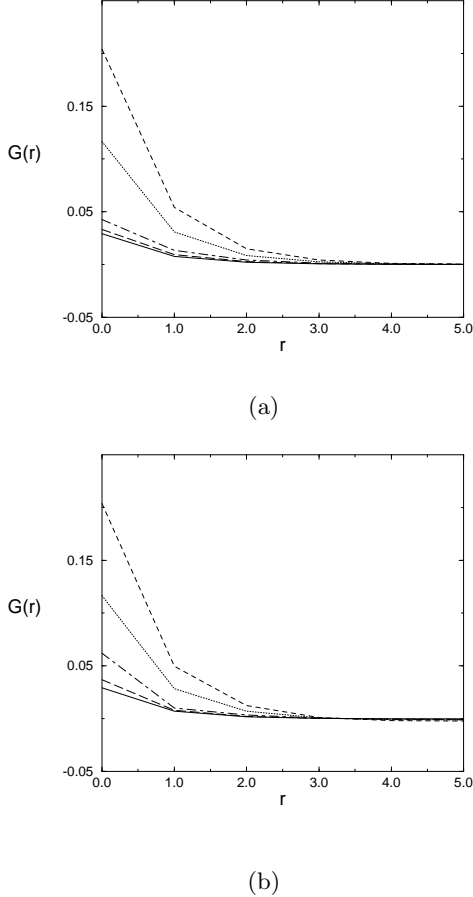


Fig. 9. Stationary pair correlation function for the non-conserved (a) and the conserved (b) linear models for several noise intensities: only additive noise with $\epsilon = 0.1$ (solid line), $\epsilon = 0.4$ (dotted line) and $\epsilon = 0.7$ (dashed line), additive ($\epsilon = 0.1$) and multiplicative noises with $\sigma^2 = 0.2$ (long dashed line) and $\sigma^2 = 0.5$ (dotted-dashed line). In all cases $a = -2$ and $D = 1$ and for the conserved case $\phi_0 = 0$.

Figure 10 shows numerical and theoretical results for $G'_0 = (G_1 - G_0)/\Delta x$ in two different cases, the linear model with only additive noise and with both additive and multiplicative noises. Empty symbols are simulation results: squares correspond to different additive noise intensities (bottom axis) and $\sigma^2 = 0$, and triangles correspond to different multiplicative noise intensities (top axis) and fixed additive noise $\epsilon = 0.1$. Lines are the theoretical prediction (Eq. (32)). We have to note that our theoretical prediction uses the simulation result for G_0 .

4.2 Conserved model

Following the same scheme as in the previous section, we now analyze the same phenomena for the conserved model. By linearizing Eq. (20) with only additive noise around $\phi(\mathbf{r}, t) = 0$, we obtain

$$\frac{\partial \phi(\mathbf{x}, t)}{\partial t} = -\nabla^2 [a\phi + D\nabla^2\phi] + \eta(\mathbf{x}, t), \quad (33)$$

where a must be negative and the additive noise is given by Eq. (21). The corresponding dynamical equation for the pair correlation function is

$$\frac{\partial G(\mathbf{r}, t)}{\partial t} = -\nabla^2 [2aG(\mathbf{r}, t) + 2D\nabla^2G(\mathbf{r}, t) + 2\epsilon\delta(\mathbf{r})]. \quad (34)$$

In the stationary state we have

$$aG(\mathbf{r}, t) + D\nabla^2G(\mathbf{r}, t) + \epsilon\delta(\mathbf{r}) = h \quad (35)$$

where h is a constant since the steady state is homogeneous. In the case $\phi_0 = 0$, this constant is zero [17, 26]. Comparing Eq. (35) with Eq. (25) in the stationary case, it can be seen that also in the conserved case Eq. (26) holds in $d = 1$.

In a more detailed analysis, we consider the lattice case when multiplicative noise is also present. We linearize Eq. (22) around $\phi = 0$ to obtain:

$$\frac{d\phi_i}{dt} = -\sum_k \tilde{D}_{ik} \left(a\phi_k + D \sum_j \tilde{D}_{kj} \phi_j + \phi_i \xi_k(t) \right) + \eta_i(t), \quad (36)$$

where the discrete noises $\eta_i(t)$ and $\xi_i(t)$ are Gaussian with zero mean and correlation given by Eqs. (23) and (10).

The procedure of the analysis is the same as in the non-conserved case. First we look for the dynamical equation of the two-point correlation function, which using Novikov's theorem [7], can be derived to be:

$$\begin{aligned} \frac{d}{dt} \langle \phi_i \phi_j \rangle &= \sum_s \tilde{D}_{is} \left[-a \langle \phi_j \phi_s \rangle - D \sum_k \tilde{D}_{sk} \langle \phi_k \phi_j \rangle + \right. \\ &\quad \left. \sigma^2 \sum_k \frac{\delta_{sk}}{\Delta x^d} \left(\tilde{D}_{sk} \langle \phi_k \phi_j \rangle + \tilde{D}_{jk} \langle \phi_k \phi_s \rangle \right) \right] + \\ &\quad \sum_s \tilde{D}_{js} \left[-a \langle \phi_i \phi_s \rangle - D \sum_k \tilde{D}_{sk} \langle \phi_k \phi_i \rangle + \right. \\ &\quad \left. \sigma^2 \sum_k \frac{\delta_{sk}}{\Delta x^d} \left(\tilde{D}_{sk} \langle \phi_k \phi_i \rangle + \tilde{D}_{ik} \langle \phi_k \phi_s \rangle \right) \right] - 2 \frac{\epsilon \tilde{D}_{ij}}{\Delta x^d}. \quad (37) \end{aligned}$$

We now focus on the stationary state $\frac{d}{dt} \langle \phi_i \phi_j \rangle = 0$ and consider the case $i = j$

$$\begin{aligned} 2 \sum_s \tilde{D}_{is} \left[a \langle \phi_i \phi_s \rangle + D \sum_k \tilde{D}_{sk} \langle \phi_k \phi_i \rangle + \epsilon \frac{\delta_{is}}{\Delta x^d} \right. \\ \left. - \sigma^2 \sum_k \frac{\delta_{sk}}{\Delta x^d} \left(\tilde{D}_{sk} \langle \phi_k \phi_i \rangle + \tilde{D}_{ik} \langle \phi_k \phi_s \rangle \right) \right] = 0, \quad (38) \end{aligned}$$

where the additive noise term has been introduced inside the Laplacian. This equation is satisfied if each term inside the Laplacian is equal to a constant h .

$$a\langle\phi_i\phi_s\rangle + D \sum_k \tilde{D}_{sk}\langle\phi_k\phi_i\rangle + \epsilon \frac{\delta_{is}}{\Delta x^d} - \sigma^2 \sum_k \frac{\delta_{sk}}{\Delta x^d} \left(\tilde{D}_{sk}\langle\phi_k\phi_i\rangle + \tilde{D}_{ik}\langle\phi_k\phi_s\rangle \right) = h \quad (39)$$

for any s, i . As before, for $\phi_0 = 0$, the constant h must be zero. We now take the case $s = i$. If we use definition (30) for the discrete derivative of the pair correlation function and take into account the isotropy of the system, Eq. (31), we can obtain from Eq. (39)

$$G'_0 = -\frac{a G_0 \Delta x}{2d D} - \frac{2\sigma^2 G_0}{D \Delta x^{d+1}} - \frac{\epsilon}{2d D \Delta x^{d-1}} - \frac{h \Delta x}{2d D}, \quad (40)$$

which in the continuous limit $\Delta x \rightarrow 0$ and in absence of external fluctuations ($\sigma^2 = 0$) coincides with the continuous analysis of Eq. (26) for $d = 1$. Notice that the dependence on the additive noise intensity is the same as in the non-conserved model, while the effect of multiplicative noise is different. Both results can be made to coincide if the intensity of the multiplicative noise of the non-conserved model A, σ_A^2 is related to the one of the conserved model B, σ_B^2 , by the relation $\sigma_A^2 = (2d/\Delta x^2)\sigma_B^2$. This relation between both models in presence of multiplicative noise has been established in several analyses [15, 17].

Again, we have performed simulations of Eq. (36) with $a = -2$ and $D = 1$ for $\phi_0 = 0$ with only additive noise, and with both white additive and multiplicative noises in a one dimensional lattice of mesh size $\Delta x = 1$ and $N = 16384$ cells. We have used a first-order Euler algorithm with time step $dt = 5 \cdot 10^{-3}$. Results for different cases of the stationary correlation function are shown in Fig. 9(b). When only additive noise is present, the pair correlation function of both conserved and non-conserved models coincide [cf. Fig. 9(a)]. As in the non-conserved case, the contribution of additive noise is here more important than the corresponding to multiplicative noise.

Analytical and numerical results for G'_0 are shown in Fig. 10. Full symbols are the simulation results in this case: squares correspond again to different additive noise intensities (bottom axis) with $\sigma^2 = 0$, and triangles to different multiplicative noise intensities (top axis) with fixed additive noise $\epsilon = 0.1$. Lines are the corresponding theoretical predictions [Eq. (40) with $h = 0$] using the values of G_0 obtained from the simulations.

5 Conclusions

In this paper we have studied the dynamics of phase ordering that appears in a non-potential situation induced by external noise. We have considered both non-conserved (order-disorder) and conserved (phase-separation) situations. Concerning the time evolution of the characteristic

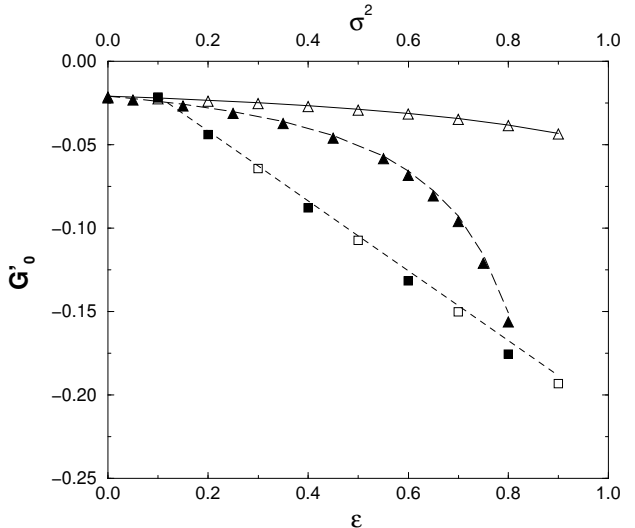


Fig. 10. Discrete first derivative G'_r of the pair correlation function in the stationary state at $r = 0$ for both non-conserved and conserved models with $a = -2$ and $D = 1$. Symbols are simulation results for both the non-conserved (empty symbols) and the conserved models (full symbols) and lines are the theoretical predictions. Squares correspond to different additive noise intensities ϵ (bottom axis) with $\sigma^2 = 0$ and triangles to different multiplicative noise intensities σ^2 (top axis) with fixed additive noise $\epsilon = 0.1$. For the conserved model we have taken $\phi_0 = 0$.

size $R(t)$ of the domains, our results indicate that $R(t)$ grows with time as a power law. The exponent of the power law is $1/2$ for the non-conserved case and $1/3$ for the conserved case. These two values coincide with the equivalent ones obtained in the decay towards an *equilibrium* state (either deterministic or in the presence of internal fluctuations). We have found a scaling description consistent with the fact that $R(t)$ is the only relevant length scale of the system, similarly also to the equilibrium cases. Moreover, the corresponding scaling functions are in agreement with the ones observed in the decay towards equilibrium. These results indicate that the physical mechanisms underlying noise-induced phase-ordering processes are identical to the deterministic ones, namely interface curvature in the non-conserved case, with the addition of diffusion in the conserved situation [27]. Finally, we have analyzed in detail a non-smooth, non-scaling behaviour induced by fluctuations that appears in the pair correlation function at short distances. We have shown that this behaviour is due to fluctuations in the bulk, and provided a theoretical expression for its magnitude.

6 Acknowledgements

This work has been supported by the Dirección General de Enseñanza Superior e Investigación Científica (Spain), under projects PB94-1167, PB96-0241, PB97-0141-C02-01, and PB98-0935. M.I. also acknowledges the Dirección

General de Enseñanza Superior e Investigación Científica for financial support.

26. M.A. Muñoz, U. Marini and R. Cafiero, *Europhys. Lett.* **43**, 552 (1998).
27. P. Pelc , *Dynamics of Curved Fronts*, Persp. in Physics, Academic Press, San Diego, 1988.

References

1. J.D. Gunton, M. San Miguel, and P.S. Sahni, in *Phase transitions and critical phenomena* vol. 8, ed. by C. Domb and J.L. Lebowitz (Academic Press, New York, 1983).
2. K. Binder and D. Stauffer, *Phys. Rev. Lett.* **33**, 1006 (1974).
3. J.L. Lebowitz, J. Marro and M.H. Kalos, *Acta. Metall.* **30**, 290 (1982).
4. M. San Miguel and R. Toral, in *Instabilities and nonequilibrium structures VI*, ed. by E. Tirapegui (Kluwer Academic, 1998).
5. M.C. Cross and D.I. Meiron, *Phys. Rev. Lett.* **75**, 2152 (1995); C. Josserand and S. Rica, *Phys. Rev. Lett.* **78**, 1215 (1997); M. Tlidi, P. Mandel and R. Lefever, *Phys. Rev. Lett.* **81**, 979 (1998).
6. R. Gallego, Ph.D. Thesis, University of the Balearic Islands (2000), available at <http://www.imedea.uib.es/PhysDept/publicationsDB>.
7. J. Garc a-Ojalvo and J.M. Sancho, *Noise in Spatially Extended Systems* (Springer, New York, 1999).
8. J. Garc a-Ojalvo, J.M. Sancho, and L. Ram rez-Piscina, *Phys. Lett. A* **168**, 35 (1992); J. Garc a-Ojalvo and J.M. Sancho, *Phys. Rev. E* **49**, 2769 (1994).
9. C. Van den Broeck, J.M.R. Parrondo, and R. Toral, *Phys. Rev. Lett.* **73**, 3395 (1994); C. Van den Broeck, J.M.R. Parrondo, R. Toral, and R. Kawai, *Phys. Rev. E* **55**, 4084 (1997).
10. J. Garc a-Ojalvo, A. Hern ndez-Machado, and J.M. Sancho, *Phys. Rev. Lett.* **71**, 1542 (1993); J. Garc a-Ojalvo and J.M. Sancho, *Phys. Rev. E* **53**, 5680 (1996).
11. J. Garc a-Ojalvo, A.M. Lacasta, F. Sagu s, and J.M. Sancho, *Europhys. Lett.* **50**, 427 (2000).
12. R. Gallego, M. San Miguel and R. Toral, *Phys. Rev. E*, to appear (2000).
13. P.C. Hohenberg and B.I. Halperin, *Rev. Mod. Phys.* **49**, 435 (1977).
14. A. Becker and L. Kramer, *Phys. Rev. Lett.* **73**, 955 (1994); *ibid.*, *Physica D* **90**, 408 (1995).
15. J. Garc a-Ojalvo, A.M. Lacasta, J.M. Sancho and R. Toral, *Europhys. Lett.* **42**, 125 (1998).
16. C. Van den Broeck, J.M.R. Parrondo, J. Armero, and A. Hern ndez-Machado, *Phys. Rev. E* **49**, 2639 (1994).
17. M. Iba es, J. Garc a-Ojalvo, R. Toral and J.M. Sancho, *Phys. Rev. E* **60**, 3597 (1999).
18. E. Oguz, A. Chakrabarti, R. Toral and J.D. Gunton, *Phys. Rev. B* **42**, 704 (1990).
19. R. Toral and A. Chakrabarti, *Comp. Phys. Commun.* **74**, 327 (1993).
20. T. Ohta, D. Jasnow and K. Kawasaki, *Phys. Rev. Lett.* **49**, 1223 (1982).
21. J.W. Cahn and J.E. Hilliard, *J. Chem. Phys.* **28**, 258 (1958); H.E. Cook, *Acta Metall.* **18**, 297 (1970).
22. R. Toral, A. Chakrabarti and J.D. Gunton, *Phys. Rev. B* **39**, 901 (1989).
23. M. Iba es, J. Garc a-Ojalvo, R. Toral, and J.M. Sancho, in *Lecture Notes in Physics*, ed. by J. Freund and T. P schel, to appear (2000).
24. R. Petschek and H. Metiu, *J. Chem. Phys.* **79**, 3443 (1983).
25. A. Chakrabarti, *Phys. Rev. B* **45**, 9620 (1992).